Journal of Fluorescence, Vol. 11, No. 2, June 2001 (© 2001)

Cytoplasmic Changes in Cardiac Cells During a Contraction Cycle Detected by Fluorescence Polarization[1]

Dror Fixler,[2] Reuven Tirosh,[2] Asher Shainberg,[3] and Motti Deutsch[2,4]

Received August 1, 2000; revised March 7, 2001; accepted March 12, 2001

Intracellular structural changes, occurring in a cardiac myocyte during a contraction cycle, were investigated by means of intracellular fluorescein fluorescence polarization (IFFP), in comparison to cytoplasmic concentration of Ca^{2+} $[Ca^{2+}]_i$ measured by indo-1. A simple physical model is presented. It assumes a biphase intracellular matrix, differing in its potency to restrict hosting fluorescent probe mobility. The first is a mobile nonrestricting phase, made mostly of aqua (aqua zone), while the second is a mobile-restricting phase, allocated mainly at the proximity of the filament sites. Their physicochemical properties such as $[Ca^{2+}]$, viscosity, and pH, may differ, thereby influencing the hosting probe fluorescence characteristics differently. These possible influences were examined experimentally. Based on experimental data, the model enables the evaluation, to first order of approximation, of the relative number of fluorescent probes populating the two phases and the time variation viscosity ($\eta_r(t)$) of the mobile-restricting filament zones taking place throughout the contraction cycle.

KEY WORDS: Cardiac myocyte; ion concentration; indo-1; intracellular Ca^{2+}.

INTRODUCTION

Fluorescence polarization (FP) is commonly used as a measure of the degree of mobility of the fluorescent marker. It is defined as $FP = (I_{\parallel} - I_{\perp})/(I_{\parallel} + I_{\perp})$, where $I_{\parallel}$ and $I_{\perp}$ are the intensities of the parallel and perpendicular components of the emitted fluorescence respectively, measured relative to the excitation electric field vector. The more restricted the fluorescent probe mobility, the higher the FP, which can theoretically be 0.5 for a randomly oriented ensemble [15,22].

Some parameters which dictate the mobility restriction level of the probe are the temperature (low) and viscosity (high) of the probe hosting media, its size, its moment of rotational inertia, binding or wobbling in a cone, and the flexibility of the binding site.

Steady-state FP measurement of fluorescent marker-labeled macromolecules enabled the study of their mobility in solution as well as their orientation in ordered biological systems such as muscle and membrane [4,45,50,52,53]. Furthermore, the fluorophore rotational motion during the time scale of its fluorescence or phosphorescence lifetime [9,28,31] can be interpreted by means of FP decay measurements.

The above-cited articles as well as many others, are based on models which assume two states of fluorescent labeling: (a) covalent binding of the probe to, or its incorporation into, the muscle fiber or membrane components of interest [4,8,49,53] and (b) embedding of the probe into a fiber or membrane component microcone-like cage, which defines the degree of the probe's orientation con-

[1] Abstract presented at the ISAC XX International Congress held at Montpellier, France, on 22–25 May 2000.

[2] The Jerome Schottenstein Cellscan Center for Early Detection of Cancer, Physics Department, Bar-Ilan University, Ramat-Gan 52900, Israel.

[3] Faculty of Life Sciences, Bar-Ilan University, Ramat-Gan 52900, Israel.

[4] To whom correspondence should be addressed. Fax: 972-3-5342019. E-mail: d__m@netvision.net.il; cellscan@albert.ph.biu.ac.il.

1053-0509/01/0600-0089$19.50/0

straint [2,28]. Hence, while enhancing our understanding of events occurring in submicroorganelles, these studies, unfortunately, to a certain extent, do not reflect the entire phenomenon of activation occurring in the intact muscle cell.

In the present article intracellular structural changes taking place during cardiac contraction are assessed by means of FP measurements and their derived analytical expressions. Such an investigation calls for the utilization of a non-covalently bound or noncaged fluorescent marker such as fluorescein diacetate (FDA). Being electrically neutral, FDA, a nonfluorescent compound, easily penetrates the cell membrane. Intracellularly, it is enzymatically hydrolyzed by a nonspecific esterase to a noncovalently bound or noncaged fluorescent fluorescein. At physiologic pH, fluorescein holds one negative surplus charge. As a result, the FDA influx rate is higher than that of fluorescein efflux, yielding intracellular accumulation of the latter [38].

Transmembrane stimulation of lymphocytes and other cells at the G_0–G_1 resting phase results in a cascade of early events, well known in the stimulation of nerve and muscle cells. These include membrane potential depolarization associated with Na^+ influx and pH changes, followed by influx and/or internal release of Ca^{2+} ions. These ionic changes activate various cytosolic ATPases and are regulated by multiple phosphorylation–dephosphorylation pathways [16].

Processes linking such early and late intracellular events following cell activation involve conformational changes of the cytosolic enzymes and/or their regulatory proteins, and their intracellular matrix reorganization [7,29]. These early structural changes may be monitored by FP of intracellular fluorescent probes [12,15,19, 51,52].

Our previous studies [27,43,54,55] indicate that intracellular fluorescein fluorescence polarization (IFFP) is an activation parameter. Consequently, it is suggested here that since an immediate effect of lymphocyte stimulation may generally be considered as cellular activation, a similar and repeatable decrease in IFFP may be expected upon contractile stimulation of a muscle fiber. This possibility was verified in this study by IFFP measurements following electrical stimulation of contraction cycles of single rat cardiac myocytes in culture.

THEORY

Solvent effects can be dramatic, and a complete change of the spectroscopic nature of a fluorescent solute can occur with a change of the solvent. The cellular matrix is a heterogeneous and polyphasic medium-solvent, in which physicochemical properties such as microviscosity, dielectric constants, polarity, and pH differ between its microdomains.

Therefore, the following is assumed.

a. Intracellular fluorescein molecules might represent an ensemble of different fluorophores, which probe different cellular regions. In such a case the steady-state IFFP is intensity weighted and given as

$$\mathrm{IFFP} = \sum i_j P_j / \sum i_j \qquad (1)$$

where i_j and P_j are the local intensity and FP of specific cellular domains denoted j, respectively.

b. For first order of approximation and for the sake of brevity, a biphase intracellular matrix muscle is assumed, differing by its potency to restrict hosting fluorescent probe mobility. One is the mobile nonrestricting phase, made mostly of aqua (aqua zone). This does not contribute to the intracellular alteration of mobile restriction. The second is the mobile-restricting zone, allocated mainly at the proximity of the filament sites (filament zone—a thought which is justified later) of the intracellular medium. It is therefore assumed that the observed FP changes occurring along the contraction cycle are due solely to changes in the mobile-restricted zone.

c. Following cell disruption the mobile-restricted fluorescein molecules become free, possessing the same spectroscopic characteristics as the mobile nonrestricted probes.

d. The relative number of fluorescent probes populating a given zone, as well as their spectroscopic characteristics, does not change during the contraction cycle (an assumption which is justified experimentally later). There is no movement of the probe from one compartment to another.

Now, let N_f, Q_f, and I_f and N_r, Q_r, and I_r, be the number, the fluorescence quantum yield, and the emitted fluorescence intensity ($\mathrm{FI} = I_{\parallel} + 2I_{\perp}$) of the intracellular free (f) probes, allocated at the aqua zone, and those of the mobility-restricted (r) probes, allocated at the filament zone, respectively. Then the total emitted intracellular FI (defined as I_C) is

$$I_C = I_r + I_f \propto N_r Q_r + N_f Q_f = N_r Q_r (1 + N\Phi) \qquad (2)$$

where $N = N_f/N_r$ and $\Phi = Q_f/Q_r$.

After cell disruption (D), the mobility-restricted noncovalently bound probes are released. In such a case the total FI (defined as I_D) is

$$I_D \propto (N_r + N_f)Q_f = N_rQ_r(1 + N)\ \Phi \qquad (3)$$

Dividing Eq. (2) by Eq. (3) gives

$$I_C/I_D = (\Phi^{-1} + N)/(1 + N)$$

from which the ratio, N, of free-to-mobility-restricted probes is extracted:

$$N = (I_C/I_D - \Phi^{-1})/(I - I_C/I_D) \qquad (4)$$

According to Eq. (1) the integrated IFFP measured from intact muscle cell will be the sum of the intensity-weighted FP (P_r and P_f) of each of the two intracellular matrix phases. This should hold true for all time points, from relaxation till complete contraction. Since neither Φ nor N changes along the contraction cycle, then

$$P_{total}(t) = \frac{I_rP_r(t) + I_fP_f}{I_r + I_f} = \frac{P_r(t)}{1 + N\Phi} + \frac{P_f}{1 + (N\Phi)^{-1}} \qquad (5)$$

In practice, utilizing Eq. (5) in the analysis of IFFP measurements of FDA labeled cells, P_f can be neglected since $P_f \ll P_r$. Obviously, this approach (as independently might be expected) dictates that $P_r(t)$ is the only component that one may expect to contribute to the time dependency of $P_{total}(t)$. For given values of N and Φ, $P_r(t)$ can be calculated from the measured $p_{total}(t)$ for all time points:

$$P_r(t) \cong (1 + N\Phi)P_{total}(t) \qquad (6)$$

In fact, FP for the free (P_f) or for the restricted (P_r) probe is determined by only three factors: the fundamental or limiting FP, P_0, which would be obtained if no disorientation followed the excitation; the rotational correlation time (τ_R) of the fluorescent probe; and its actual fluorescence decay time (τ_F). The relation among these three parameters and the measured P is given by the Perrin [36] equation:

$$1/P - 1/3 = (1/P_0 - 1/P)(1 + \tau_F/\tau_R) \qquad (7)$$

τ_R reflects influences of environmental parameters such as temperature, viscosity, mobility, and probe binding upon rotational diffusion. For a spherical probe, it equals $\eta V/RT$, where η is the viscosity of the solvent, V is the molar volume of the fluorescent probe, R is the gas constant, and T is the absolute temperature.

τ_F may decrease with respect to τ_{F0}, the fundamental fluorescence lifetime, due to various environmental processes which compete with fluorescence in depopulating the excited states. Thus, the fluorescence quantum yields, $Q = \tau_F/\tau_{F0}$, of free ($Q_f = \tau_F^f/\tau_{F0}$) and mobility-restricted ($Q_r = \tau_F^r/\tau_{F0}$) probes (even of the same fluorescent molecule) are expected to be different.

While some of the simple fluorescent probes, weighing a few hundred daltons, may be considered to come close to "rigid spheres," those which are bound to or caged by macromolecules as well as fluorescent molecules of the biological specimens cannot always be assumed to have both of these characteristics. The motion of the latter two can no longer be characterized by a single value of τ_R but by three, a fact which makes Eq. (7) much more complicated [5,18,37,51].

Nevertheless, fluorescein is a <300-Da molecule. Its longest side is built up of three aromatic rings of about 15-Å length. Thus, for fluorescein as well as fluorophores similar in their dimensions, the dependency $1/P(T/\eta)$, as given by Eq. (7), is generally correct. Hence, IFFP measurements of FDA-labeled cells can be analyzed by means of Eq. (7), yielding quite accurate results.

This approach permits a direct and simple expression arrived at by the extraction of $1/P$ from Eq. (7) and its introduction into the reciprocal of Eq. (6):

$$\begin{aligned}\frac{1}{P_{total}(t)} &= \frac{1}{P_r(t)}(1 + N\Phi) \\ &= \left[\left(\frac{1}{P_0} - \frac{1}{3}\right)\left(1 + \frac{\tau_F}{\tau_R(t)}\right) + \frac{1}{3}\right](1 + N\Phi) \\ &= \left[\frac{\tau_F}{\tau_R(t)}\left(\frac{1}{P_0} - \frac{1}{3}\right) + \frac{1}{P_0}\right](1 + N\Phi) \\ &= \left\{\left(\frac{T}{\eta(t)}\right)\left(\frac{1}{P_0} - \frac{1}{3}\right)\frac{R\tau_F}{V} + \frac{1}{P_0}\right\}(1 + N\Phi) \qquad (8)\end{aligned}$$

which suggests that when τ_F is independent of the contraction cycle, the time dependency of IFFP [$P_{total}(t)$] is due mostly to the time variation viscosity $\eta_r(t)$ of the mobile-restricting filament zones.

MATERIALS AND METHODS

Cell Culture

Cell culture of cardiac myocytes from rat hearts was prepared as described previously [20]. Briefly, rat hearts (1–2 days old) were removed under sterile conditions and washed three times in phosphate-buffered saline (PBS) to remove excess blood cells. The hearts were minced to small fragments and then agitated gently in a solution of proteolytic enzymes, RDB (Biological Institute, Ness-Ziona, Israel), which was prepared from a fig tree extract. The RDB was diluted 1:50 in Ca^{2+}- and Mg^{2+}-free PBS at 25°C for a few cycles of 10 min each, as described previously [20]. Dulbecco's modified Eagle's medium (DMEM) containing 10% horse serum (Biological Indus-

tries, Beit Haemek, Israel) was added to supernatant suspensions containing dissociated cells. The mixture was centrifuged at 300*g* for 5 min. The supernatant phase was discarded, and the cells were resuspended. The suspension of the cells was diluted to 1×10^6 cells/ml, and 1.5 ml was placed in 35-mm plastic culture dishes on collagen/gelatin-coated coverglasses. The cultures were incubated in a humidified atmosphere of 5% CO_2, 95% air at 37°C. Confluent monolayers exhibiting spontaneous contractions were developed in culture within 2 days. The growth medium was replaced after 24 h and then every 3 days.

Sample Preparation for Measurements

For electrical stimulation measured by IFFP and indo-1, cells were grown on a microscope coverslip, which was installed in a specially designed measurement chamber, containing connectors for electrodes. The chamber was then fixed on a Zeiss inverted epifluorescence microscope stage equipped with a xenon lamp. The illuminated field was confined to approximately the cross section of a single cardiac myocyte, which were observed to yield stable contractions in response to electrical stimulation.

Electrical Stimulation

Stimulation was carried out at the frequency range of 0.1 to 1 Hz, with a pulse duration and strength of about 1 ms and 40 V, respectively.

Cell Staining

Cell staining procedures with FDA or with indo-1/AM were similar and were carried out directly on the measurement chamber as follows: 100 μl of staining solution of a 2 μ*M* marker (FDA, Sigma, St. Louis, MO; indo-1/AM, Molecular Probes, I-1203), dissolved in modified Dulbecco's PBS (PBS + 1.2 m*M* Ca^{2+} + 1.2 m*M* Mg, 280 mosmol), was introduced onto the cultured cells in the chamber. After 5 min of staining at room temperature, the cells on the coverslip were meticulously rinsed three times with PBS to remove extracellular marker.

Fluorescence Measurements

To perform both microscopic IFFP and indo-1 ratiometric (*R*) measurements, the Zeiss inverted epifluorescence microscope was upgraded electronically and optically. For IFFP measurements, excitation was carried out at 470 nm, and fluorescence was measured at 520 ± 10 nm. Changes in the intracellular concentration of free calcium, $[Ca^{2+}]_i$, were traced by ratiometric FI measurements at 405 and 495 nm of indo-1-labeled free calcium which was excited at 345.5 nm (Grynkiewitz, 1985).

Comparison and calibration measurements were made on a Perkin Elmer spectrofluorimeter, Model MPF-44, with FP measurement capabilities, using glycerin–PBS solutions of various viscosities and fluorescein concentrations. Lifetime measurements were carried out using the ISS-K2 spectrofluorimeter at a modulation frequency range of 5–200 MHz.

All fluorescence measurements were carried out at 23°C.

Cell Disruption

For measurement of I_D, cells and their organelles were disrupted directly in the measurement chamber by sonication with a Sonifer B-12 apparatus (Branson Sonic Power Co., Danbury, CT) for about 15 s. After sonication, no intact cells or their fractions could be observed using light microscopy. To prevent a possible rise of temperature caused by sonication, the measurement chamber, containing the cells, was maintained in ice during the sonication procedure.

RESULTS

Measurement of IFFP and *R* During a Single Cardiac Myocyte Contraction

Figure 1 shows a representative chart of the IFFP(*t*) ranging from about 0.220 to 0.170), *R*(*t*), intracellular

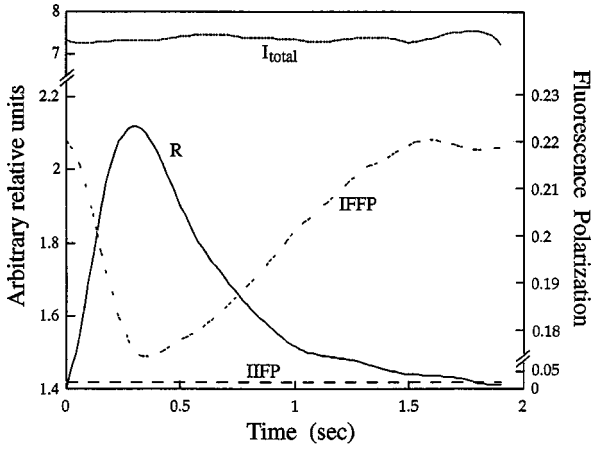

Fig. 1. Representative charts of IFFP(*t*), *R*(*t*), IIFP(*t*), and I_{total}, recorded along a single cardiac myocyte contraction cycle. Fluorescence intensity and ratio relate to the left-hand scale, while IFFP and IIFP relate to the right-hand scale.

indo-1 FP [IIFP(t)], and FI (I_{total}) of fluorescein, all recorded along a single cardiac myocyte contraction cycle. The data indicate a reciprocal relation with a slower decay time of IFFP(t) compared to $R(t)$. Furthermore, $I_{total}(t)$ seems to be constant, suggesting that no emigration of fluorescein occurs during the contraction cycle from the filament zone to the aqua zone, and vice versa. As a consequence, N_f,N_r, and N are independent variables of the contraction cycle, supporting supposition d under Theory. IIFP was found to be approximately zero, similar to values of FP obtained in water using either fluorescein or indo-1.

Estimation of N, the Ratio of Mobile Nonrestricted:Restricted Molecules

Estimation of N required FI measurements before (I_C) and after (I_D) cell disruption. This was carried out using an objective with a low numerical aperture (NA = 0.25 × 20), to collect light from a field of about 30 cells and their surroundings. In this way, the number of fluorescein molecules, observed in the measured field before and after disruption, stays constant; therefore changes in FI can be related exclusively to the solute/solvent interaction, and not to dye dilution, which might occur due to sonication.

Cells on the microscope coverslip, covered with PBS, were first brought in focus using transmitted light. Then, without changing the focus, the PBS solution was replaced with a staining solution by gentle pipetting. After 5 min, the staining solution, containing extracellular fluorescein, was meticulously rinsed out of the chamber and replaced with a PBS solution and the I_C was measured. The cells were then disrupted and a measurement of I_D was taken.

I_C and I_D may vary between experiments since the dye concentration cannot be totally controlled due to the dilution occurring during solution replacement.

Figure 2 shows the results of seven such measurements of I_C, I_D, their ratio, their corresponding N calculated according to Eq. (4), and P_D, the FP of the disrupted cell mixture. As shown in Fig. 2, despite the fact that the absolute values of I_C and I_D vary, I_D/I_C, N, and P_D remain constant and equal: 1.25 ± 0.011, 0.43 ± 0.054, and 0.026 ± 0.002, respectively.

Estimation of the Viscosity $\eta_r(t)$

Using Eq. (8), the constancy of Φ, N, and P_0 and knowledge of $P_r(t)$ during the contraction cycle are not enough to extract the corresponding estimated time response curve of $\eta_r(t)$, since neither τ_F^r nor V is known.

Thus, for first-order estimation of $\eta_r(t)$, the calculated $P_r(t)$ values are compared to those of fluorescein fluorescence polarization (FFP) measured in glycerol–water solutions of given viscosities as follows (see Fig. 3). First, the reciprocal of FFP versus T/η for glycerol–fluorescein water solutions of different viscosities is depicted. Then, a horizontal line, originating at a given $1/P_r(t)$ value, is drawn. The $T/\eta_r(t)$ value of the intersection point is the desired one.

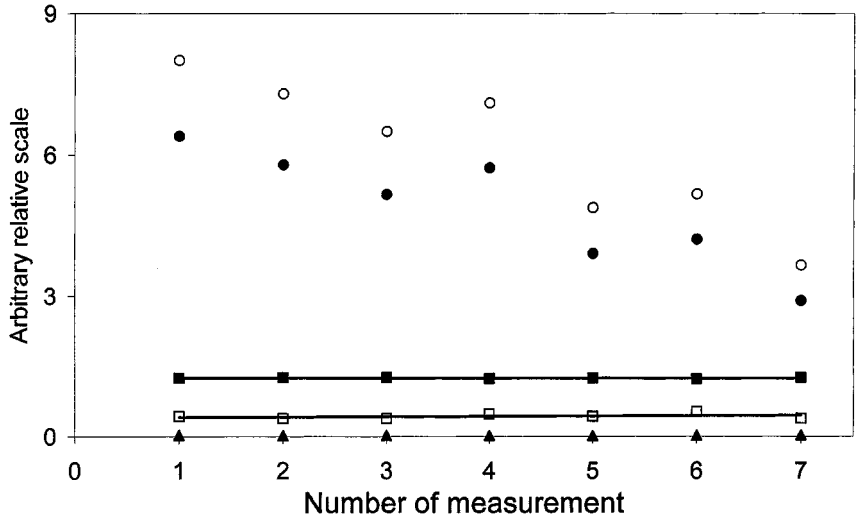

Fig. 2. Estimation of N: seven representative measurements (performed five times at each point) of I_C (●), I_D (○), their ratio I_D/I_C (■), their corresponding N (□) calculated according to Eq. (4), and fluorescein P_D(▲).

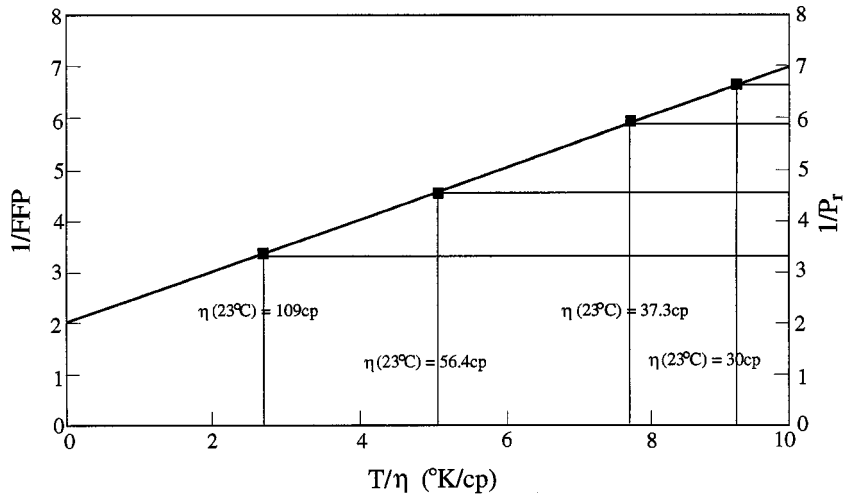

Fig. 3. First-order estimation of $\eta_r(t)$ by comparing the calculated $P_r(t)$ values to the FFP values. First, the reciprocal of FFP versus T/η for glycerol–fluorescein water solutions of different viscosities is depicted (thick diagonal line). Then, a horizontal line (thin solid line), originating at a given $1/P_r(t)$ value, is drawn. The $T/\eta_r(t)$ value of the intersection point (■) is the desired one.

Figure 4 depicts representative curves of $T/\eta_r(t)$ and $R(t)$ of a single contraction cycle. Each data point is the outcome of averaging over 10 contraction cycles per each time point. During hundreds of repeated experiments, the peak value of $R(t)$ was found to precede that of $T/\eta_r(t)$ by less than 100 ms. Moreover, a shorter rise time and relaxation time of $R(t)$ than of $T/\eta_r(t)$ were also noted.

τ_F and FFP Dependence on $[Ca^{2+}]_i$

To investigate the possible and direct influence of parameters which change during the contraction cycle ($[Ca^{2+}]_i$, pH, viscosity) upon IFFP, measurements were carried out free of perturbations arising in heterogeneous cellular medium, in homogeneous solutions.

To examine the possibility of whether alternations of

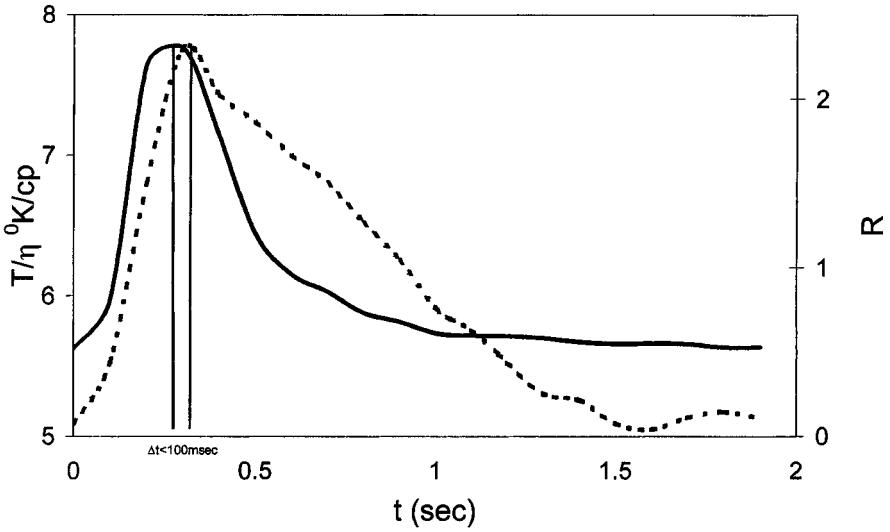

Fig. 4. Representative curves of $T/\eta_r(t)$ (dashed line) and $R(t)$ (solid line) of a single contraction cycle measured at 23°C. Each data point is the outcome of averaging over 10 contraction cycles per time point. The standard deviation is smaller than 5% and is not depicted.

IFFP along the contraction cycle are induced by a direct influence of Ca^{2+}, FFP was measured in fluorescein (2 μM)–glycerol (50%) aqueous solutions in PBS with varying Ca^{2+} concentrations. The results (shown in Fig. 5) indicate the independence of FFP in Ca^{2+} and, as a result, also that of τ_F in accordance with Eq. (7), over a very broad range of concentrations (nanomolar to millimolar).

The Ca^{2+}-free solution (control) had a neutral pH, 7.4, and the addition of Ca^{2+} did not change the solution pH. An exception was the higher concentration of 1 m*M*, where the pH decreased to 7.1, in agreement with other published results [1,47]. Nevertheless, the latter did not affect FFP, in agreement with the following experiments.

τ_F and FFP Dependence on pH

One might suspect that $P_r(t)$ is not an independent parameter, but only reflects variation of the intracellular pH (pH_i) occurring along the contraction cycle, resulting in changes in τ_{F0} as well as in τ_F^r, due to solute/solvent interaction [21]. To investigate the influence of pH on τ_F and FFP, three solutions of fluorescein (2 μM)–glycerol (40%) in PBS were prepared, having pH values of 6.12, 7.3, and 8.2 (far wider than the pH range of change occurring during contraction [33].

FFP and lifetime were measured for each solution at least in triplicate. Each experiment lasted 5 min, using 5- to 200-MHz modulation frequencies. For all solutions, only one component of τ_F was found. The results depicted in Fig. 6 indicate that, in the range of 6–8 pH units in a viscous aqueous solution and at room temperature, FFP is independent of pH (under the measuring system sensitivity limitations), while τ_F is poorly pH dependent (a slope of about 4%).

τ_F and FFP Dependence on Viscosity

One of the more clear influences of viscosity upon a hosting fluorophore is the shortening of its fluorescence decay time [21]. In the following, the question of whether the obvious dependence of $P_r(t)$ on $\eta_r(t)$ might be enhanced due to shortening of τ_F^r, as a result of $\eta_r(t)$, was examined.

Using the same measurement setup and procedures described in the above section, the dependency of both τ_F and FFP on η were measured in fluorescein (2 μM)–glycerol (40%) in PBS having a neutral pH, 7.4. Viscosity was determined by controlling the solution temperature (to better than 0.01°C). The results, obtained at four temperature measuring points, are presented in Fig. 7. While only one component of τ_F was found, equal to 3.95 $\pm$ 0.01 ns and temperature independent, FFP was found to be reciprocally temperature dependent.

DISCUSSION

The measured time–response curve of IFFP along the cardiac cycle covers a broad range of rather high FP values, from about 0.230 to 0.170. The calculated values of P_r, according to Eq. (6), are even higher—0.350 to 0.253—suggesting a significant level of mobility restriction, forced upon the probe by its intracellular environment. In general this restriction can be related to either

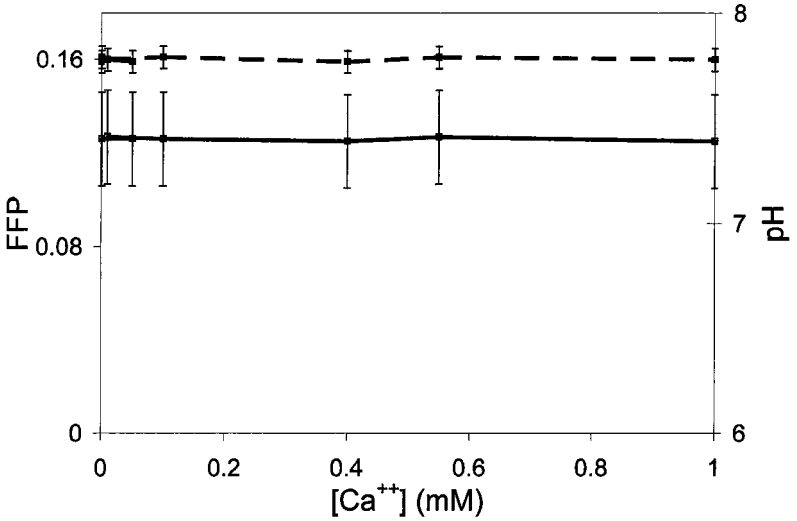

Fig. 5. FFP (dashed line) and pH (solid line) dependency upon Ca^{2+} concentration as measured in glycerol–fluorescein water solutions at 23°C.

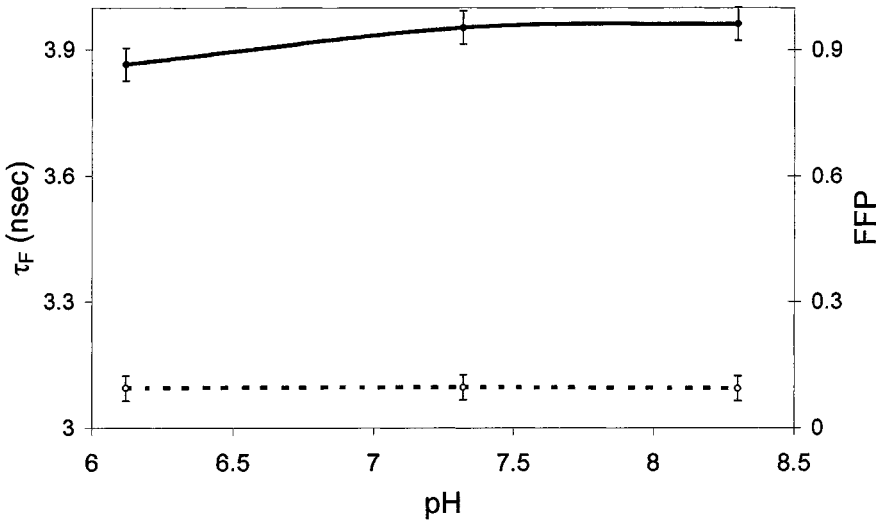

Fig. 6. FFP (dashed line) and τ_F (solid line) versus pH as measured in glycerol–fluorescein water solutions at 23°C.

solvent structure or viscosity (friction-like) restrictions. The central mechanisms behind the solvent structure mobility restriction are covalent binding, attachment of dye molecules to macromolecules due to dipole–dipole interactions, or even higher orders of charge arrangements, caging, and "wobbling-in-cone" [14,31].

Other well-established cellular parameters (such as pH, $[Ca^{2+}]$, η, and temperature increase due to heat production associated with the contraction process), which seem to alternate simultaneously with IFFP during the contraction cycle, might influence IFFP either directly or indirectly through their possible influence upon τ_F.

In light of the present study, our previous work, and the work of others, the different mechanisms are discussed below.

The Physical Nature of Fluorescein–Cellular Medium Interaction in FDA-Labeled Cells

FP measurements of ultrasonically disrupted, FDA-labeled cardiac myocytes showed a negligible FP value (~0.02; see Fig. 2), as in PBS. This is in complete agreement with results obtained with both FDA- and carboxyfluorescein diacetate (CFDA)-labeled PBL [14], but in

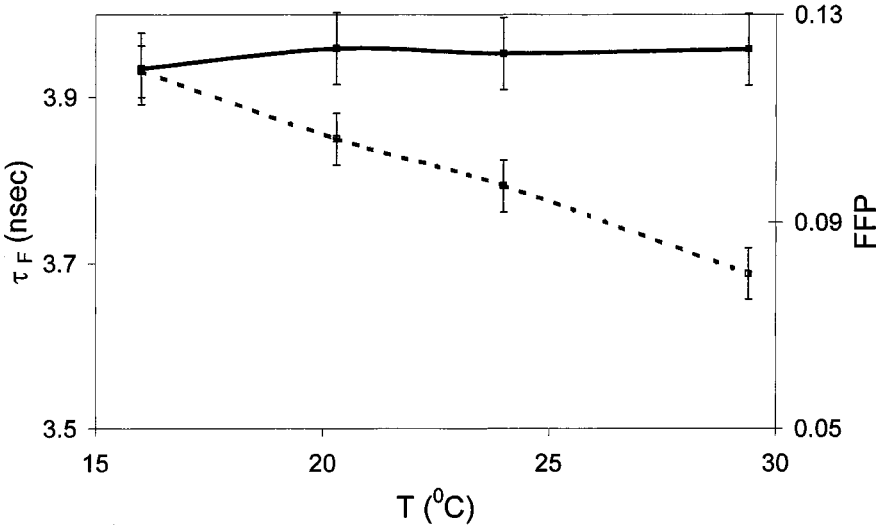

Fig. 7. FFP (dashed line) and τ_F (solid line) dependency upon viscosity as measured in glycerol–fluorescein water solutions. The viscosity was determined by controlling the solution temperature (to better than 0.01°C).

contrast to results obtained with 2,7-bis-carboxyethyl-5(6)-carboxyfluorescein/acetoxymethyl- ester (BCECF/AM)-labeled PBL, which showed a rather high level of FP (~0.2) following disruption [23].

The origin of these differences seems to be primarily the fact that in a physiological environment, fluorescein and CF correspondingly hold one and two surplus negative charges, while BCECF holds four or five [44]. This is further supported by the fact that both intracellular fluorescein and CF leak out of the cell more easily than BCECF [14,42]. These results indicate that while at least part of the intracellular BCECF is bound to sites on macromolecules or strongly associated with them, fluorescein and CF seem to be nonbinding but mobile-restricted solutes within the cytosol, sensing their local viscosity.

In both cases, the status of intracellular dye shares the common characteristic of an ~3- to 7-nm fluorescence red shift [23]. Red-shifted emission may indicate different levels of the extensiveness of solute/solvent interaction, not necessarily due to electrostatic solvent effect, and relying solely upon solute binding. The reason for such emission shifts in nonbinding solvents can be several: pH, polarity, polarizeability, viscosity, etc.

In most polar aromatic molecules whose lowest single states are (π,π^*), the excited state is more polar than the ground state [25]. Therefore, the excited molecules tend to interact with polar solvents so as to align the solvent dipoles. This alignment decreases the energy of the excited state and causes the emission spectra to shift toward the red. This generally holds true even when both solvent and solute are not polar, since excitation induces electrostatic polarization [11].

Interestingly enough, in the case of fluorescein, the red shift increases as the solvent polarity decreases [32]. The cellular content has a polarity lower than that of the suspending PBS solution. This might further explain the red shift of intracellular fluorescein compared to that of fluorescein in disrupted FDA-labeled cell solutions. Hence, it is believed that solvent polarity, rather than tight binding, is the dominant reason behind the phenomenon of red shift, a conclusion which is strengthened in light of the results obtained in both leakage and disruption experiments of FDA-labeled cells.

This supports the approach that in FDA-labeled cells fluorescein indeed senses an intracellular "Perrin-like" matrix. This, together with the fact that unbound fluorescein can be related to a spherical probe, enables the utilization of the Perrin formula [Eq. (7)] for extraction of viscosity values from the calculated P_r values. Nevertheless, following Perrin, the legitimacy of such a calculation might be enhanced if the τ_F and temperature do not change significantly during the contraction cycle. The following corroborates these possibilities.

The Effect of Ca^{2+} on FFP and τ_F

The earliest detectable alterations of biochemical components occur milliseconds following exposure of the cell to the relevant stimulating agent, whether chemical or electrical [40]. $[Ca^{2+}]$ is such a prominent component. Following stimulation, a rapid influx of Ca^{2+} occurs, usually accompanied by a release of intracellular sarcoplasmic reticulum Ca^{2+} and resulting in a transient rise in free cytoplasmatic $[Ca^{2+}]_i$ which lasts, at most, a few seconds in cardiac myocytes [39,40].

During the contraction cycle of cardiac myocyte, $[Ca^{2+}]_i$ is transiently changed from about 100 to 800 n*M* [13], with a time–response curve which was found in this study to be similar to the time dependence behavior of the reciprocal of IFFP(t) and $\eta_r(t)$. This resemblance supports the supposition that $[Ca^{2+}]_i$, rather than $\eta_r(t)$, is the direct and even the sole parameter determining the observed IFFP(t) taking place along the contraction cycle. However, the results shown in Fig. 5 negate this possibility and suggest that IFFP may be an independent parameter, which shows evidence of structural events occurring during the contraction cycle.

The Effect of pH on FFP and τ_F

pH influences the spectroscopic features of fluorescent probes, a fact which is very well established and utilized in pH_i determination [34,35,48] and for the indication of cell activation. It is one of the prominent factors which has been observed to change during the early stages of the activation process following cell stimulation.

Regarding fluorescein, FI and color variations as a function of pH are commonly related to the extent of fluorescein dissociation and ionization. Nevertheless, one might suspect that the pH_i changes following stimulation [6] as well as in cells equilibrated with buffers of increasing pH [48] will be manifested by the absorbing power and FI changes of the fluorescent probe.

These two parameters are related to the fluorescence quantum yield $Q_F = \tau_F/\tau_{F0}$. Thus, changes in FP and IFFP could be physically induced by pH changes through changes in $\tau_F = \tau_0 \cdot Q_F$. Indeed, the results depicted in Fig. 6 indicate that τ_F is poorly pH dependent (an average slope of about 4%) over the range of 6–8.5 pH units, at room temperature. However, under the measuring system sensitivity limitations used in this study, FFP was found to be independent of pH, when pH was either directly (Fig. 6) or indirectly (Fig. 5) changed. The present find-

ings therefore suggest that IFFP and pH probe different physiological effects of cellular stimulation, rather than being affected by each other.

Indirect Influence of the Viscosity on IFFP via τ_F

The estimated intracellular $\eta_r(t)$ ranges from about 37 to 56 cP along the contraction cycle (Fig. 4), in accordance with FP values and P_r as presented at the beginning of the Discussion. The FP measured in this study is within the range found by FP measurement methods for Euglene and yeast cells at 27°C, the range of the viscosity is higher (compared to 6.3 and 14 cP, respectively) [46]. The reason for this is the fact that in the studies cited, only one homogeneous intracellular bulk medium was considered, and measurements were carried out at 27°C.

One of the more obvious influences of increasing viscosity upon a hosting fluorophore is the shortening of its fluorescence decay time [21], thereby additionally but indirectly increasing FP. This phenomenon was found to be negligible in the viscosity range relevant to the present study IFFP values (see Fig. 7). Furthermore, since P is reciprocally related to τ_F [Eq. (8)], the absolute value of their relative change fulfills

$$\Delta P/P \propto \Delta\tau_F/\tau_F \tag{9}$$

Now, according to the results depicted in Fig. 7, $\Delta P/P \cong 33\%$ (a change from about 0.119 to 0.08), while $\Delta\tau_F/\tau_F \cong 0.6\%$ (a change from about 3.935 to 3.958 ns).

According to Eq. (9), such magnitudes of relative changes negate the possibility that the alterations in τ_F due to viscosity changes might have a meaningful contribution to the alteration of IFFP taking place along the contraction cycle. Thus, for any practical motivation and under the present experimental conditions, τ_F might be considered as a constant along the contraction cycle, further strengthening our model assumption (assumption d above) and understanding of Eq. (8). The physical reasoning behind these results is the fact that τ_F is poorly related to both the η and the T values relevant to this study, whereas η and, therefore, also IFFP are both exponentially temperature dependent, after Andreda [3].

In addition to the last three sections above dealing with τ_F, one should further consider the consequence of forcing upon Eq. (4) the experimental finding that I_C/I_D is constant for various values of I_C and I_D. As a result, both N and Φ also remain constant (they are independent of each other; N is an ensemble property, while Φ is a single molecule property). Hence,

$$\text{Constant} = \Phi = Q_f/Q_r = (\tau_F^f/\tau_{F0})/(\tau_F^r/\tau_{F0}) = \tau_F^f/\tau_F^r \tag{10}$$

By definition, the aqua zones are spectroscopically apathetic, suggesting the permanence of τ_F^f, which in turn dictates the constancy of τ_F^r according to Eq. (10) and in agreement with the present results.

Significance of IIFP

The FP of both indo-1 and fluorescein was negligible in aqua (PBS). In glycerol–PBS solution (60% glycerol) the FP of indo-1 was found to be significantly higher than that of fluorescein (0.31 and 0.168, respectively; data not shown), while intracellularly it was found to be negligible in comparison to FFP (0.003 compared to ~0.23).

These three independent findings may suggest that (a) indo-1 is a probe less sensitive to alterations of rotational mobility restrictions (showing a higher FP than fluorescein in the same homogeneous viscous solution), and therefore, (b) it is most probably confined to the aqua phase in the cell, whereas (c) at least some of the fluorescein molecules occupy exclusively the more mobile-restricted regions and are likely to sense their η_r.

Reconstitution experiments (data not shown), performed under controlled levels of Ca^{2+} and Mg ATP on solutions demonstrated a nearly zero degree of FFP. These results were obtained in spite of the high viscous solutions of purified actin filaments or transparent gels made of collagen. Similar results were also observed in transparent collagen gels. These results are consistent with those obtained in the present study for intracellular indo-1 and fluorescein in PBS. Thus, it is suggested that fluorescein senses changes in fluidity/flexibility of the troponin–troposmyosin complex on the actin filament during the contraction cycle. This, as well as the above claims (a and b) are further strengthened in light of the fact that indo-1-labeled calcium cannot be "bound" to the troponin–troposmyosin regulatory system [26], and it is therefore reasonable to assume that it occupies the aqueous zones, yielding a low FP.

The Biophysical Aspect

In the electrically stimulated twitch contraction of cultured cardiac myocytes, rise times and decay times of $1/\eta$ were found to be longer than those of R, as shown in Fig. 4. Similar behavior was obtained when shortening was compared to $[Ca^{2+}]_i(t)$ along the contraction cycle of adult cardiac myocytes, as measured 1 h after a short exposure to indo-1/AM [41]. These results are consistent with similar measurements on ferret papillary muscle [10], where the active phase of isometric tension develop-

ment or unloaded shortening was longer than that of the $[Ca^{2+}]_i$ transient.

We therefore propose that the increase in $1/\eta$ during twitch contraction, as measured by IFFP, could probably monitor the increase in flexibility of the troponin–troposmyosin and the actin–myosin complexes, in response to calcium mobilization. This increase in flexibility during contraction may be related to a certain loosening of the regulatory complex, as inferred from the large increase in viscosity upon *in vitro* formation of the troponin–tropomyosin complex from its components in solution [17]. Indeed, it is generally accepted that the regulation of muscle contraction involves cooperative and allosteric interactions among the protein components of the muscle thin filament and myosin heads during ATP hydrolysis [30,39].

CONCLUSIONS

The main message of this study is the possible use of IFFP for monitoring and studying cardiomyocyte contraction, in comparison with the well-established Ca^{2+} probes. The IFFP(t) time–response curve indicates an alteration in the rotational freedom or fluorescence lifetime of fluorescein molecules during the contraction cycle. To get an idea about the order of magnitude of this change, an effective viscosity is considered. The cell is assumed to be a heterogeneous Perrin medium. The average IFFP values obtained are compared to those of fluorescein FP measured in glycerol–water solutions of given viscosities.

ACKNOWLEDGMENT

This work was supported by the Horwitz Foundation Grant.

REFERENCES

1. D. G. Allen and C. H. Orchard (1983) *J. Physiol (Lond.)* **355**, 555–567.
2. T. S. Allen, N. Ling, M. Irving, and Y. E. Goldman (1996) *Biophys. J.* **70**, 1847–1862.
3. E. N. da C. Andrade (1954) *Endeavour*, **12**, 117–127.
4. D. Axelrod (1979) *Biophys. J.* **26**, 557–574.
5. G. G. Belford, R. L. Belford, and G. Weber (1972) *Proc. Natl. Acad. Sci. USA* **69**, 1392–1393.
6. M. Bental and C. Deutsch (1994) *Am. J. Physiol.* **266**, C541–C551.
7. G. Berke (1989) in W. E. Paul (Ed.), *Fundamental Immunology*, Raven Press, New York, pp. 735–764.
8. J. Borejdo and S. Putnam (1977) *Biochim. Biophys. Acta* **459**, 578–595.
9. T. P. Burghardt (1985) *Biophys. J.* **48**, 623–631.
10. S. C. Calaghan and E. White (1999) *Prog. Biophys. Mol. Biol.* **71**, 59–90.
11. I. D. Campbell and R. A. Dwek (1984) *Biological Spectroscopy*, Benjamin Cummings, Menlo Park, CA, pp. 103–107.
12. S. Chaitchik, M. Deutsch, O. Asher, G. Krauss, P. Lebovich, H. Michlin, and A. Weinreb (1988) *Eur. J. Cancer Clin. Oncol.* **25**, 861–866.
13. M. Chen, H. Hashizume, C. Y. Xiao, A. Hara, and Y. Abiko (1997) *Life Sci.* **60**, PL57–PL62.
14. M. Cohen-Kashi, M. Deutsch, R. Tirosh, H. Rachmani, and A. Weinreb (1997) *Spectrochim. Acta A* **53**, 1655–1661.
15. M. Deutsch, I. Ron, A. Weinreb, R. Tirosh, and S. Chaitchik (1996) *Cytometry* **23**, 159–165.
16. M. Deutsch, N. Zurgil, M. Kaufman, and G. Berke (2000) in K. P. Kearse (Ed.), *T Cell Protocols: Development and Activation*, Humana Press, Totowa, NJ, pp. 221–242.
17. S. Ebashi and M. Endo (1968) *Prog. Biophys. Mol. Biol.* **18**, 123–183.
18. M. Ehrenberg and R. Rigler (1976) *Q. Rev. Biophys.* **9**, 69–81.
19. A. Eisenthal, O. Marder, D. Dotan, S. Baron, B. Lifschitz-Mercer, S. Chaitchik, R. Tirosh, A. Weinreb, and M. Deutsch (1996) *Biol. Cell.* **86**, 145–150.
20. D. El-Ani, K. A. Jacobson, and A. Shainberg (1994) *Biochem. Pharmacol.* **48**, 727–735.
21. P. P. Feofilov (1961) *The Physical Basis of Polarized Emission*, Consultants Bureau, New York.
22. D. Fixler, R. Tirosh, A. Eisenthal, S. Lalchuk, O. Marder, and M. Deutsch (1998) *J. Biomed. Opt.* **3**, 312–325.
23. E. Gelman-Zhornitsky, M. Deutsch, R. Tirosh, Y. Yishay, A. Weinreb, and H. M. Shapiro (1997) *Biomed. Opt.* **2**, 186–194.
24. M. Grynkiewicz, M. Poenie, and R. Y. Tsien (1985) *J. Biol. Chem.* **260**, 3440–3550.
25. G. G. Guilbault (1967) *Fluorescence: Theory, Instrumentation and Practice*, Marcel Dekker, New York, p. 77.
26. R. A. Haworth and D. Redon (1998) *Cell Calcium* **24**, 263–273.
27. M. Kaplan, E. Trebnyikov, and G. Berke (1997) *J. Immunol. Methods* **201**, 15–24.
28. K. Kinosita, S. Kowato, and A. Ikegami (1977) *Biophys. J.* **20**, 289–305.
29. A. Kupfer and G. Dennert (1984). *J. Immunol.* **133**, 2762–2766.
30. S. S. Lehrer and M. A. Geeves (1998) *J. Mol. Biol.* **277**, 1081–1089.
31. G. Lipari and A. Szabo (1980) *Biophys. J.* **30**, 489–506.
32. K. K. Meisingset and H. B. Steen (1981) *Cytometry* **1**, 272–278.
33. J. M. Metzger (1996) *Am. J. Physiol.* **270**, H1008–H1014.
34. R. F. Murphy, S. Powers, M. Verderame, C. R. Cantor, and R. Pollack (1982) *Cytometry* **2**, 402–406.
35. R. F. Murphy, S. Powers, and C. R. Cantor (1984) *J. Cell Biol.* **98**, 1757–1762.
36. F. Perrin (1929) *Ann. Phys.* **12**, 169–275.
37. F. Perrin (1936) *J. Phys. Rad.* **7**, 1–11.
38. B. Rotman and B. W. Papermaster (1966) *Proc. Natl. Acad. Sci. USA* **55**, 134–141.
39. R. J. Solaro and H. M. Rarick (1998) *Circ. Res.* **83**, 471–480.
40. M. Sonenberg and A. S. Schneider (1977) in P. Cuatrecasas and M. F. Greaves (Eds.), *Receptors and Recognition, Ser. A, Vol. 4*, Chapman and Hall, London, pp. 1–32.
41. H. A. Spurgeon, M. D. Stern, G. Baartz, S. Raffaeli, R. G. Hansford, A. Talo, E. G. Lakatta, and M. C. Capogrossi (1990) *Am. J. Physiol.* **258**, H574–H586.
42. M. Sunray, M. Deutsch, M. Kaufman, R. Tirosh, A. Weinreb, and H. Rachmani (1997) *Spectrochim. Acta Part A* **53**, 1645–1653.
43. M. Sunray, M. Kaufman, N. Zurgil, and M. Deutsch (1999) *Biochem. Biophys. Res. Commun.* **261**, 712–719.
44. J. A. Thomas, R. N. Buchsbaum, A. Zimniak, and E. Racker (1979) *Biochemistry* **18**, 2210–2218.
45. R. T. Tregear and R. M. Mendelson (1975) *Biophys. J.* **15**, 455–467.
46. S. Udenfriend, P. Zaltzman-Nirenburg, and G. Guroff (1966) *Arch. Biochem.* **116**, 261–270.

47. R. D. Vaughan-Jones, W. J. Lederer, and D. A. Eisner (1983) *Nature* **301**, 522–524.
48. J. W. M. Visser, A. A. M. Jongeling, and H. J. Tanke (1979) *J. Histochem. Cytochem.* **27**, 32–35.
49. H. Vogel and F. Jahnig (1985) *Proc. Natl. Acad. Sci. USA* **82**, 2029–2033.
50. G. Weber (1952) *Biochem. J.* **51**, 145–155.
51. G. Weber (1971) *J. Chem. Phys.* **55**, 2399–2404.
52. G. Weill and J. Sturm (1975) *Biopolymers* **14**, 2537–2553.
53. T. Yanagida and F. Oosawa (1978) *J. Mol. Biol.* **126**, 507–524.
54. N. Zurgil, M. Kaufman, and M. Deutsch (1999) *J. Immunol. Methods* **229**, 23–34.
55. N. Zurgil, Y. Levy, M. Deutsch, B. Gilburd, J. George, D. Harats, M. Kaufman, and Y. Shoenfeld (1999) *Clin. Cardiol.* **22**, 526–532.